GeoFlow Experiment - From Numerical Simulation to Experimental Data Evaluation Overall Dynamics and First Data Identification

B. Futterer & S. Koch

Dept. Aerodynamics and Fluid Mechanics,
Brandenburg University of Technology Cottbus, Germany

Topical Team
Geophysical Flow Simulation
Meeting 11/12 June 2009
BTU Cottbus

funded by: German Aerospace Center e.V. (DLR), 50 WM 0822,
European Space Agency (ESA), grant number AO99-049, ESA Topical Team, grant number 18950/05/NL/VJ

Research topics of GeoFlow in the experimental framework

- non-rotating case
  - coexistence of several flow modes (axisymmetric, cubic/octahedral, pentagonal)
  - influence of initial conditions to reach different stable states
  - transition direct from steady to irregular flow with remnant tetrahedral symmetry
- rotating case
  - change of sign for drift velocity
  - complex pattern drift
  - transition to stabilizing effects due to centrifugal forces
  - transition from steady via periodic to irregular flow

Dynamics of GeoFlow: summary in stability diagram including flow states I

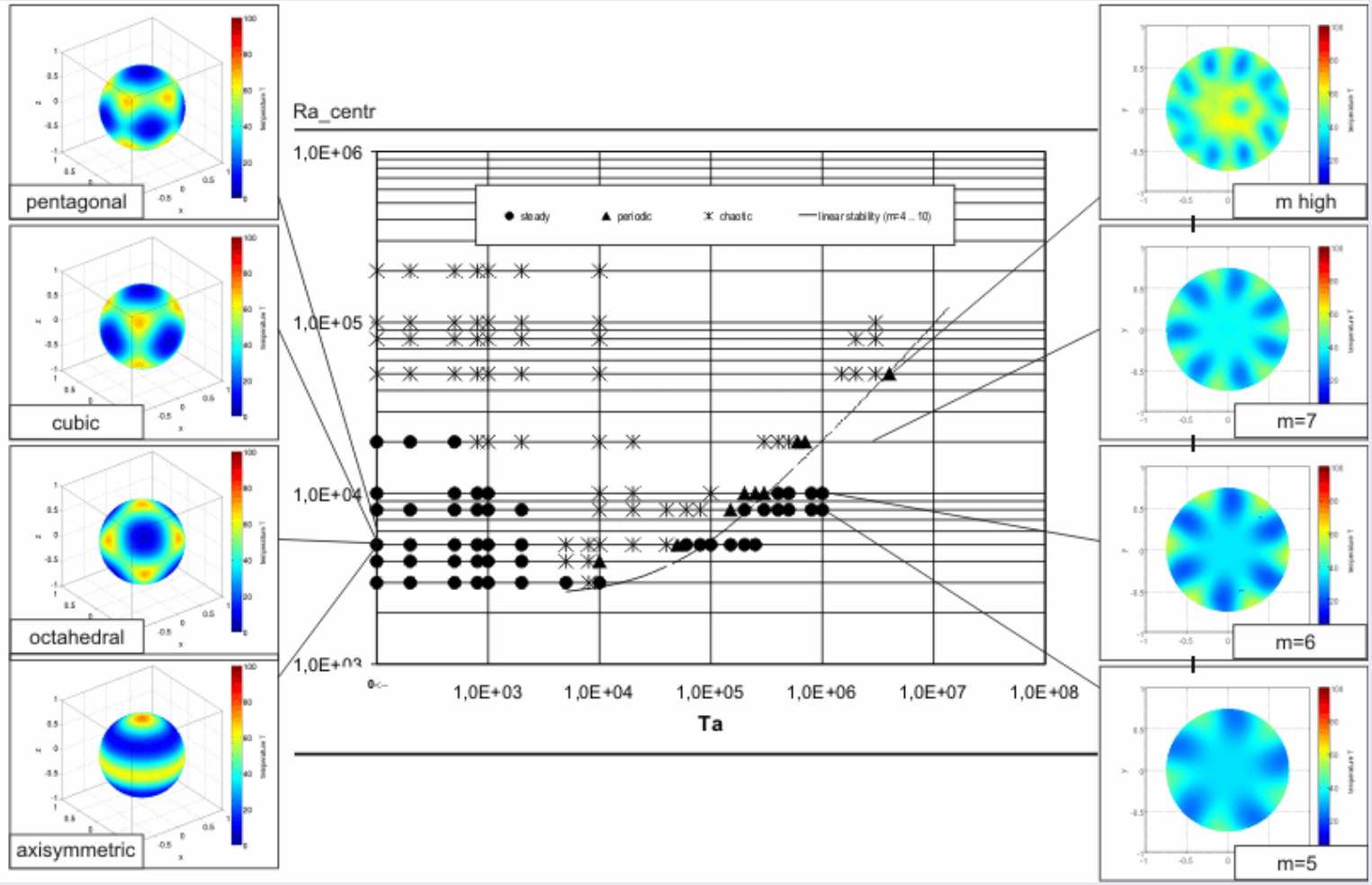

Thermal convection in non-rotating and rotating spherical shells:
Onset of time-dependence as a function of Taylor number with steady, periodic and irregularly fluctuating, i.e. chaotic solutions. The solid line denotes the critical Rayleigh numbers for highest mode of first instability in the rotating case [Travnikov et. al, 2003].

Dynamics of GeoFlow: summary in stability diagram including flow states I

- time-dependency characterized by kinetic energy and Nusselt number
  i.e. $E_{kin} = const.$ and $Nu_i = Nu_o \rightarrow$ steady
- local variables show
  - characteristics of a travelling wave for Ta low ($Ta \leq 10^4$)
    $\rightarrow$ to be confirmed finally
- shift of stability line calculated with energy method and from DNS
  - stability line marks onset of first instability
  - characteristics of Rossby waves for Ta moderate and high ($Ta > 10^4$)
    $\rightarrow$ to be confirmed finally
  - below: basic state with $Nu = 1$

Dynamics of GeoFlow: summary in stability diagram including flow states II

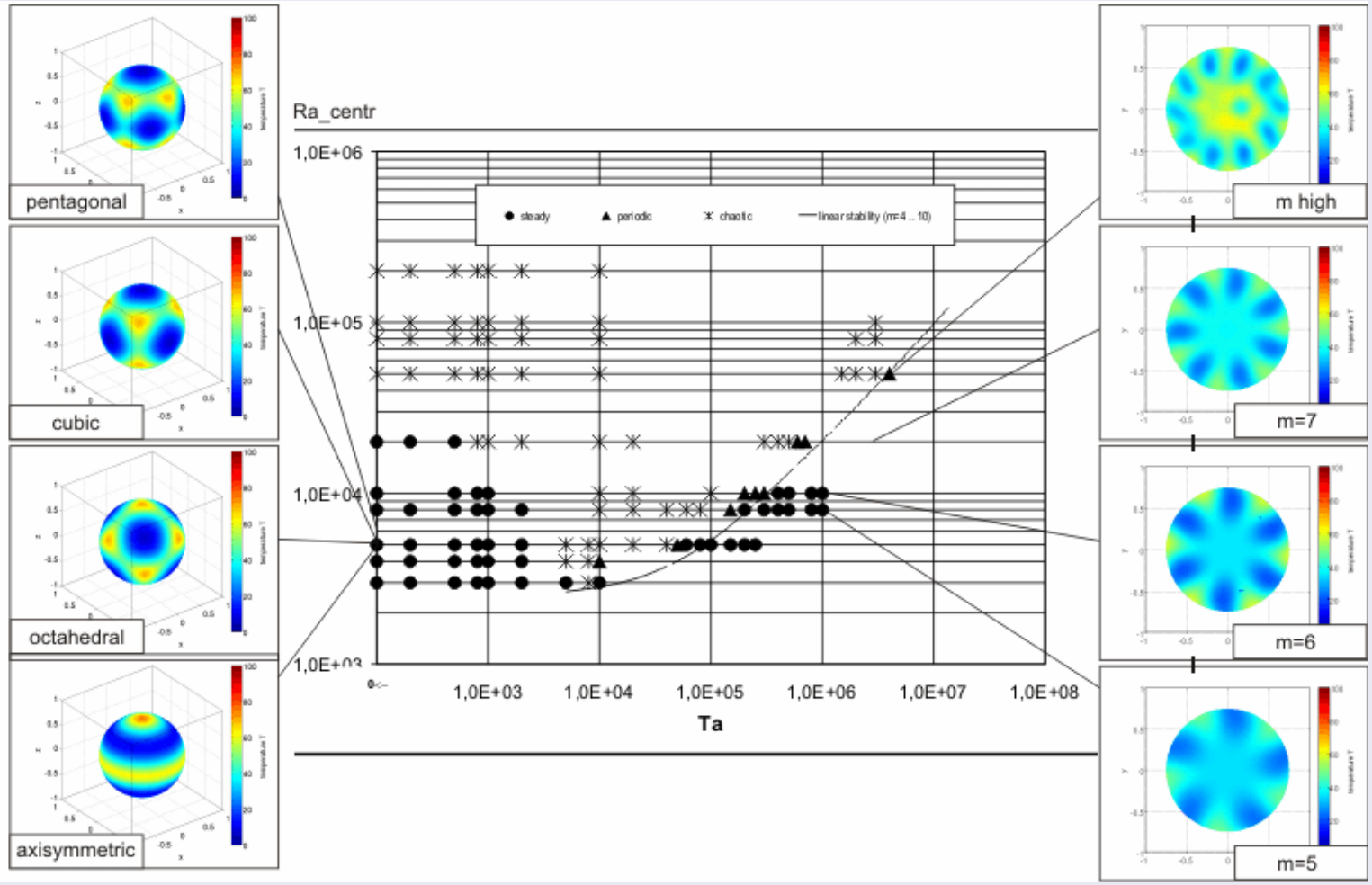

Patterns of spherical shell convection in the non-rotating case $Ta = 0$:
Visualization of temperature field in radial direction with red coloring corresponding to hot up-flow and blue coloring corresponding to cold discharge of flow.
Example of co-existing modes at $Ra_{centr} = 5 \cdot 10^3$: solutions of axisymmetric, octahedral resp. cubic, pentagonal symmetry from bottom to top.

Dynamics of GeoFlow: summary in stability diagram including flow states III

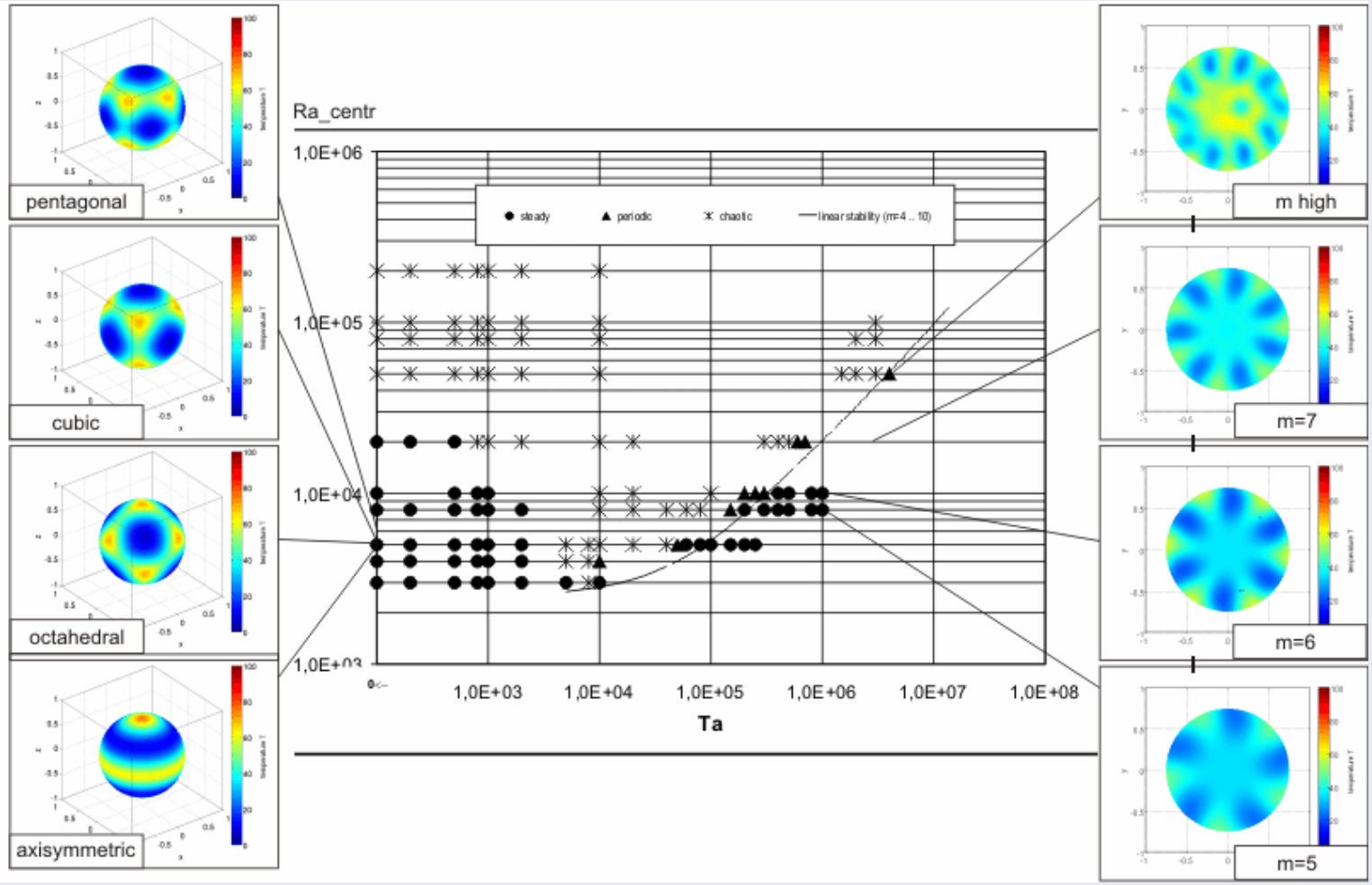

Patterns of spherical shell convection in the rotating case $Ta \neq 0$:
Visualization of temperature field with view at the top of the sphere, i.e. the middle of the image is the 'polar' region. Increasing of mode number m with increasing of parameter set. From bottom to top: $m = 5$ at $(Ra_{centr}, Ta) = (8 \cdot 10^3, 1 \cdot 10^6)$, $m = 6$ at $(1 \cdot 10^4, 1 \cdot 10^6)$, $m = 7$ at $(2 \cdot 10^4, 2 \cdot 10^6)$, $m = 10$ at $(5 \cdot 10^4, 4 \cdot 10^6)$.

Dynamics of GeoFlow: stability diagram from numerical simulation . . .

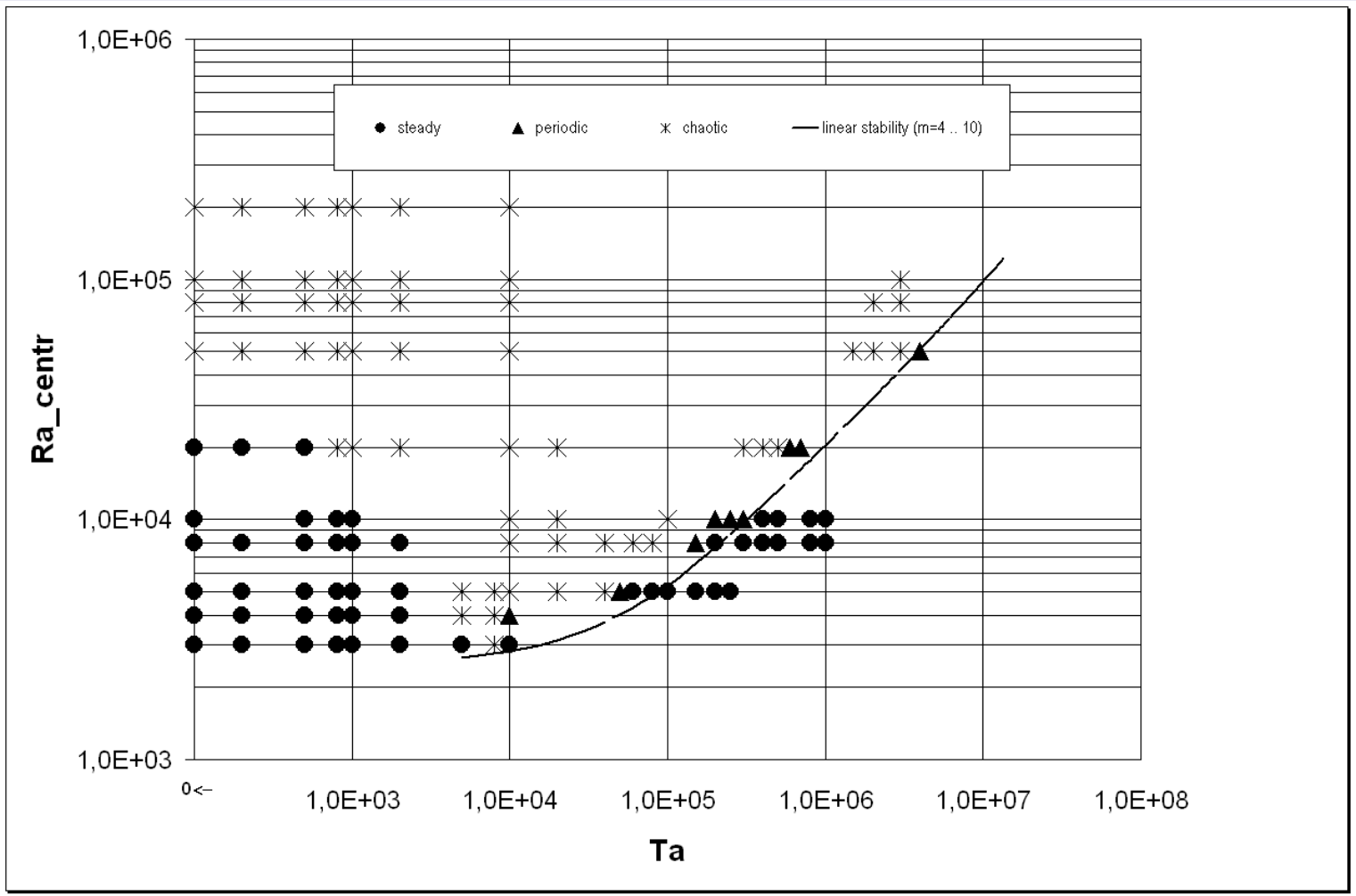

Dynamics of GeoFlow: stability diagram
. . . with all experimental runs . . .

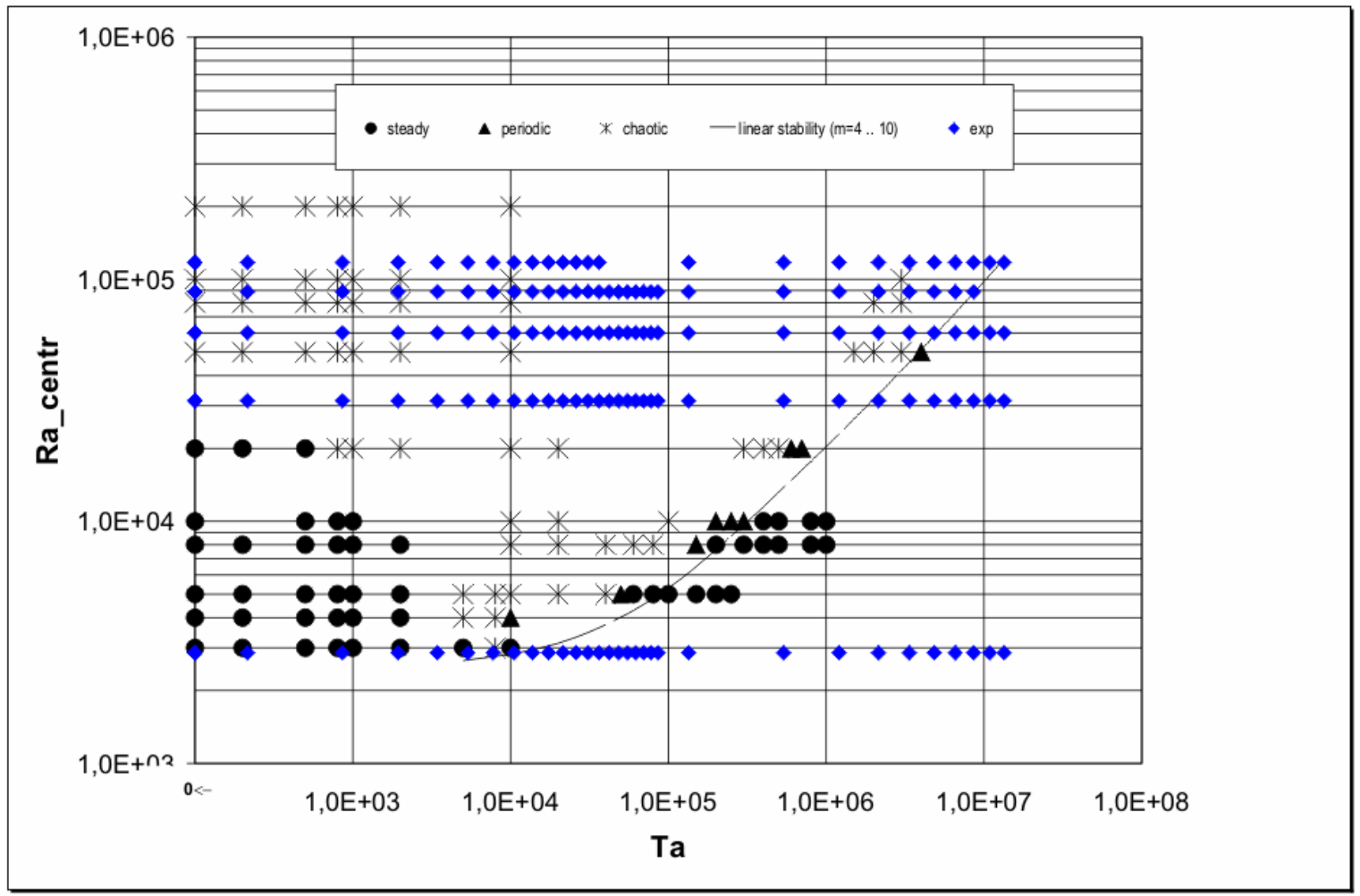

Dynamics of GeoFlow: stability diagram
. . . with specific selection for first evaluation

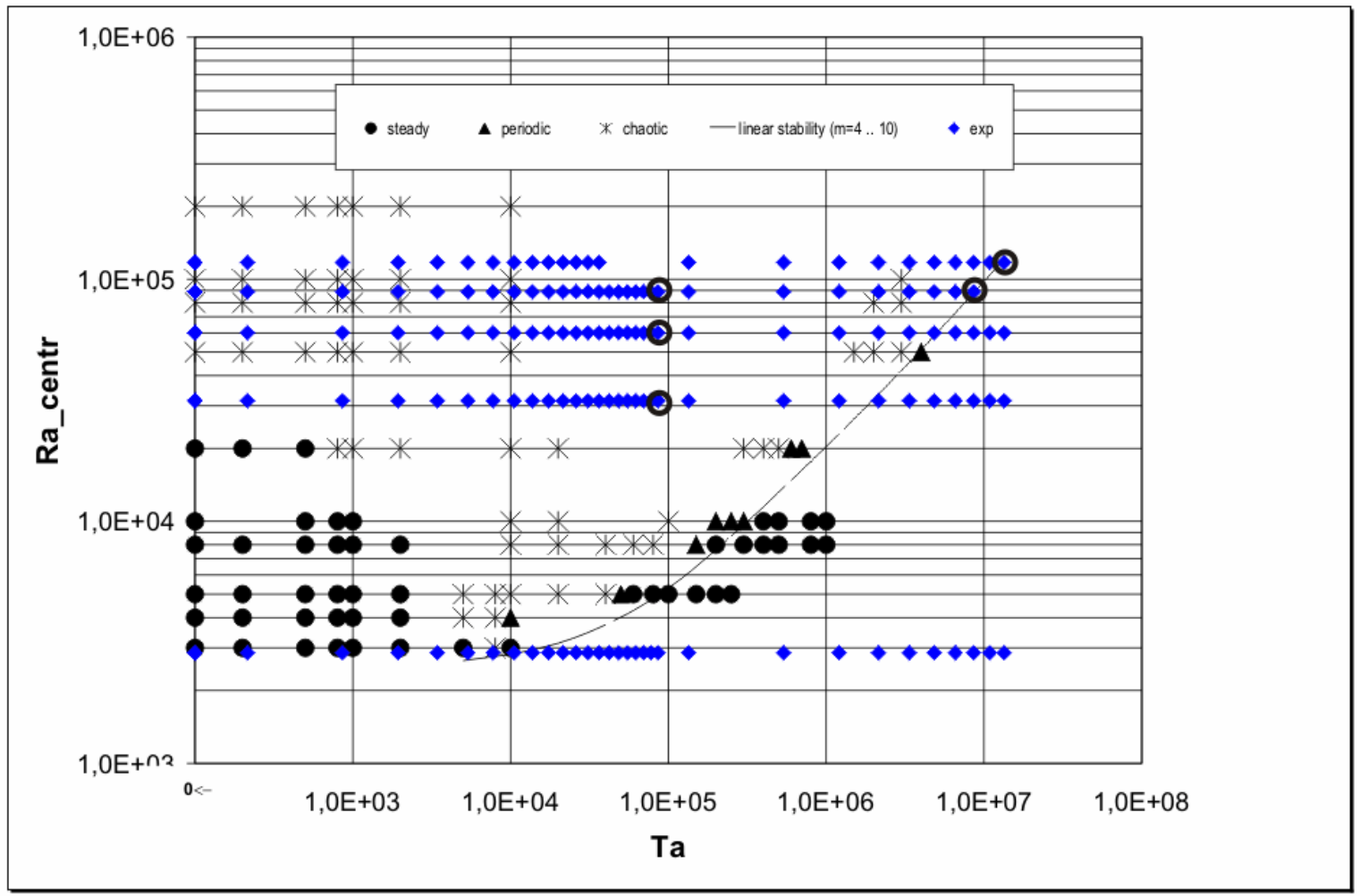

Numerical and experimental visual data analysis

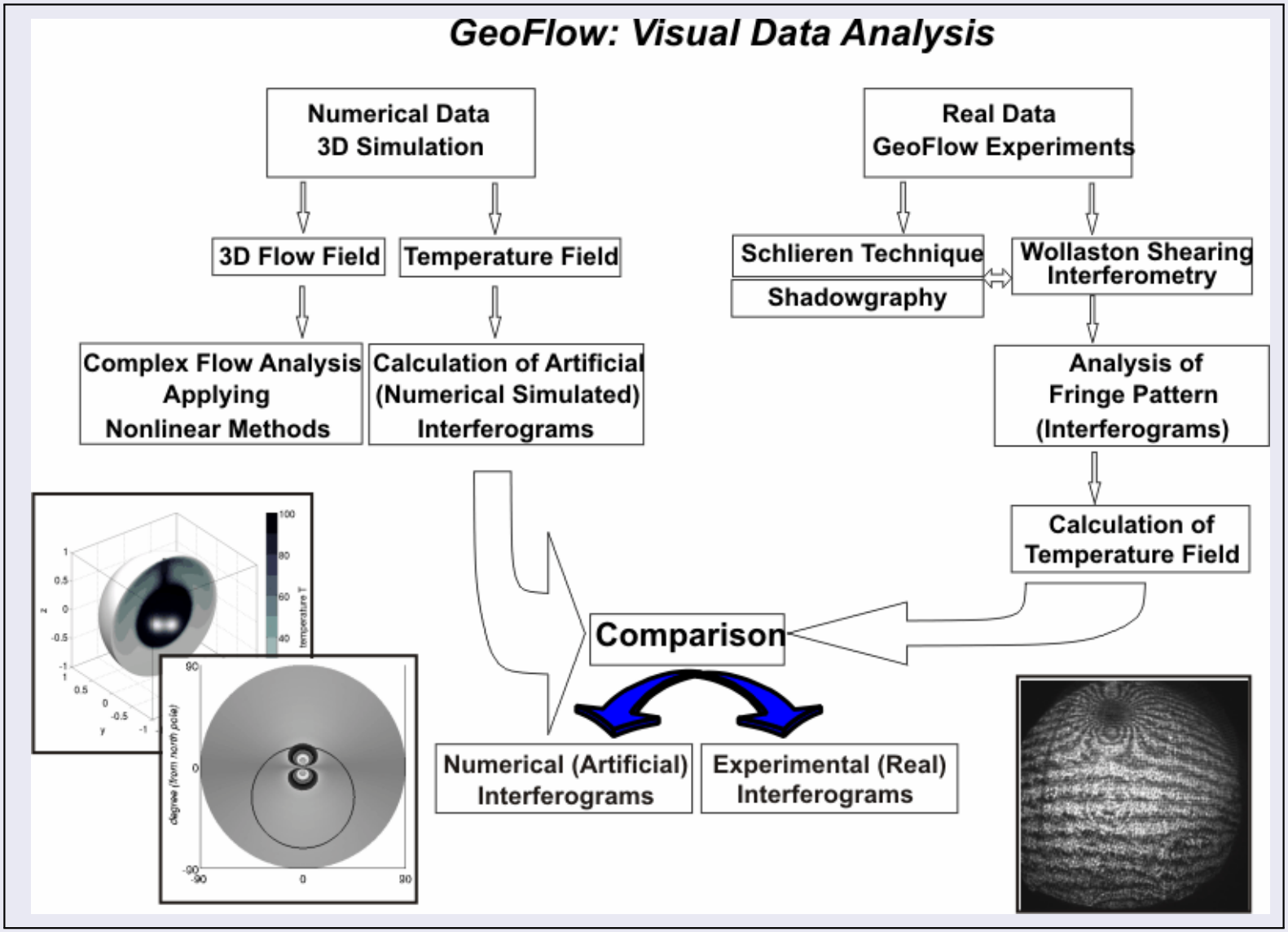

Wollaston shearing interferometry

- refractive index n=(λ,ρ,p,T)
  temperature gradient $\longrightarrow$ density gradient $\longrightarrow$ refractive index gradient
  - variation of optical path length $\longrightarrow$ interference: Wollaston shearing interferometry
  - deflection of beam: Schlieren/shadowgraphy
- modular Wollaston shearing interferometer works as Schlieren/shadowgraphy

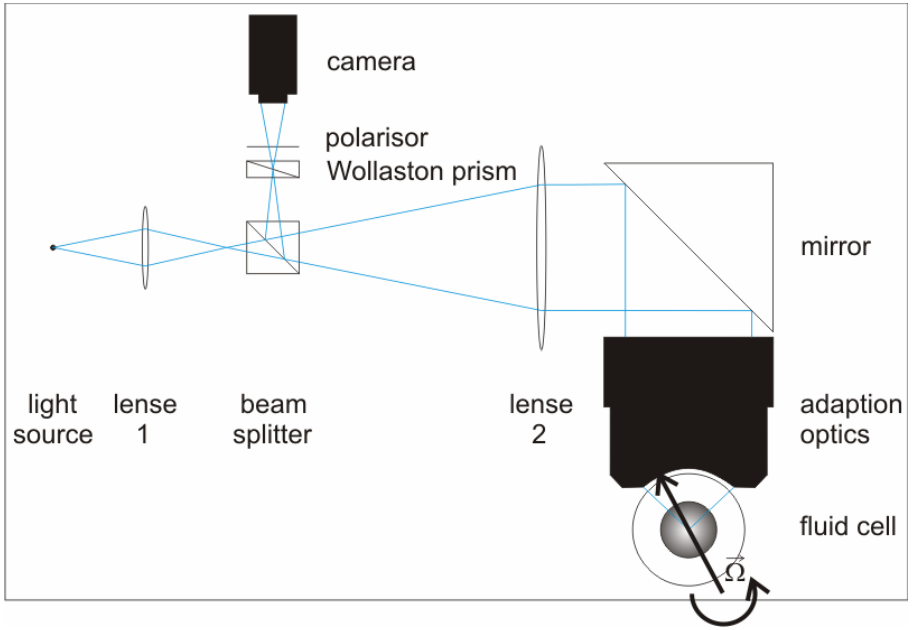

scetch of ray path

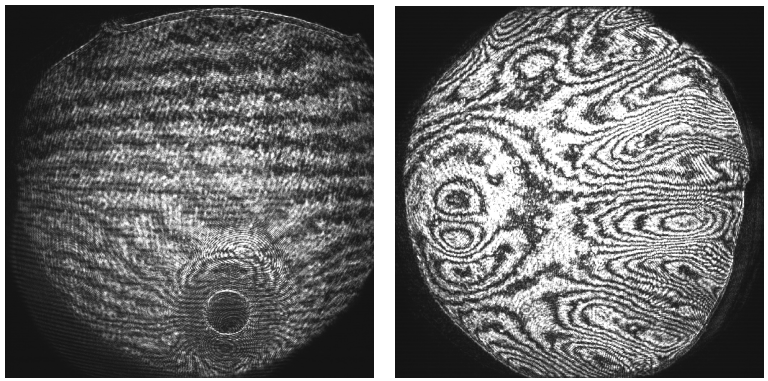

interferograms

Camera position and image view

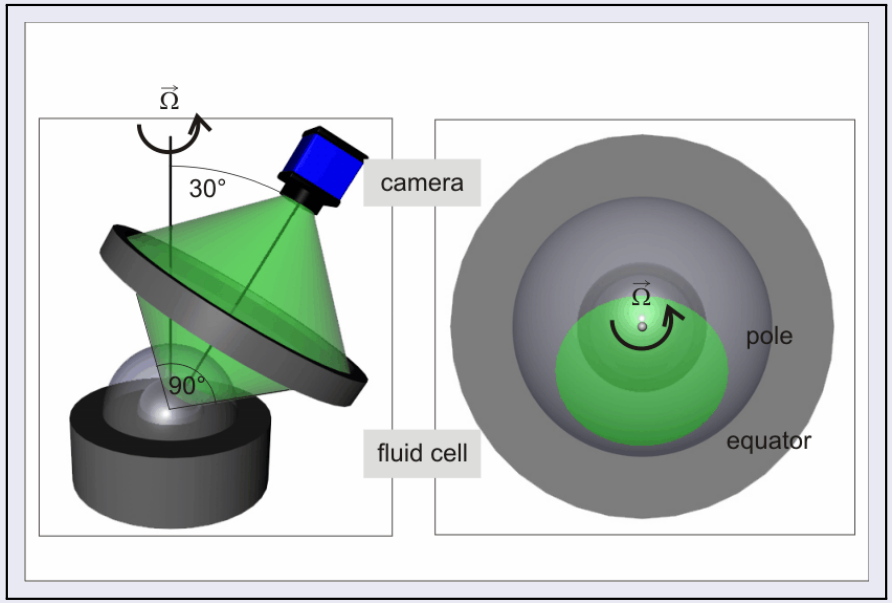

Triggering of image capture each 60°
→ 6 positions gives measurement picture of whole hemispherical surface

Data volume

images	200 GB
telemetry	50 GB

telemetry - technical values, scientific values (ΔT, μg, etc.)

Process of reconstruction of whole hemisphere in a plane

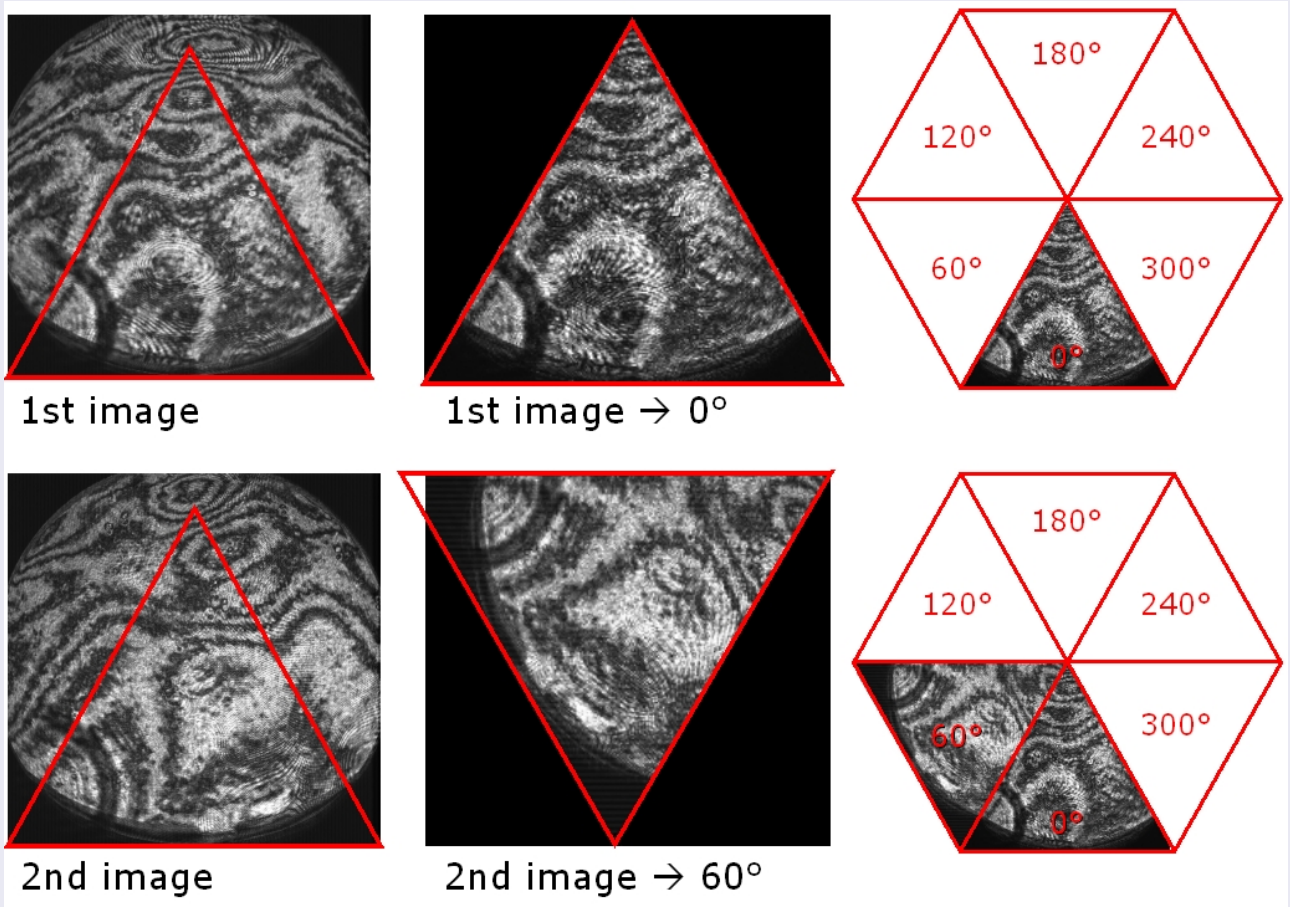

- image taken every 60° → images overlap → only a sector is visible
- defined mask (ROI) over image sequence → 6 sectors
- note: no interpolation, because of mixing fringes to gray
- note: pole is supposed to be fixed

Reconstruction of images for specific part during RUN #4

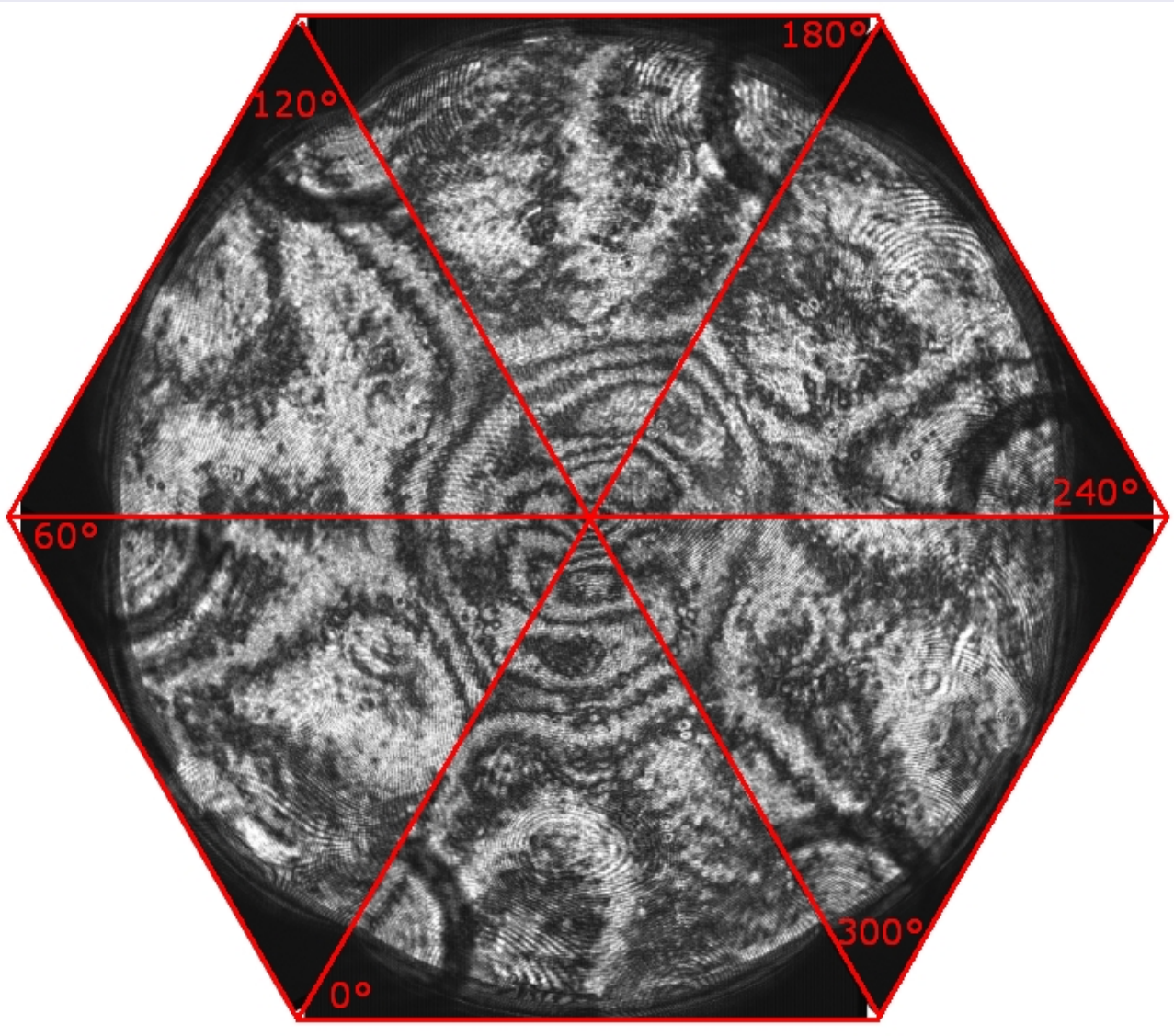

Reconstruction of images for specific part during RUN #4

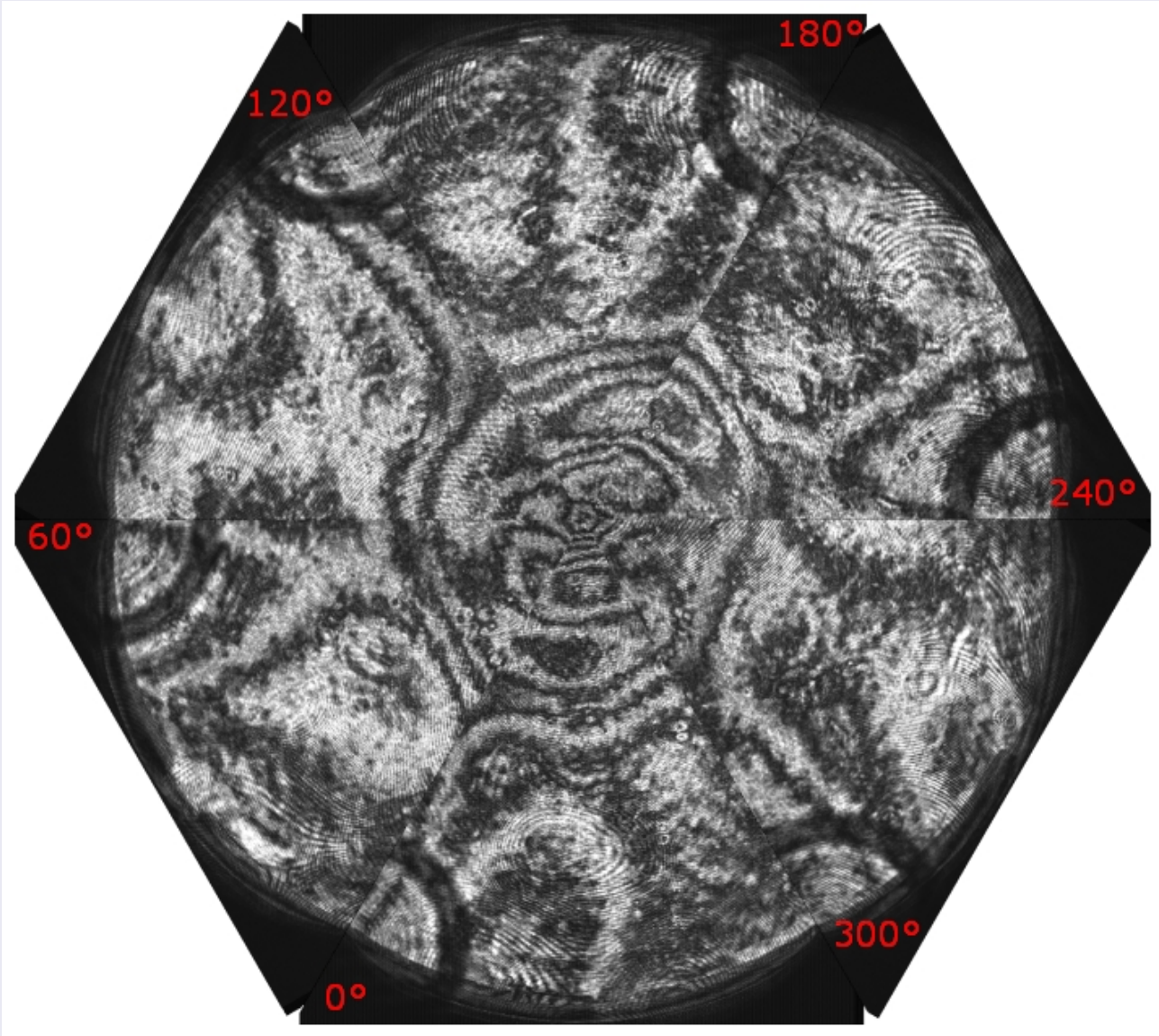

Dynamics of GeoFlow: stability diagram
. . . with specific selection for first evaluation

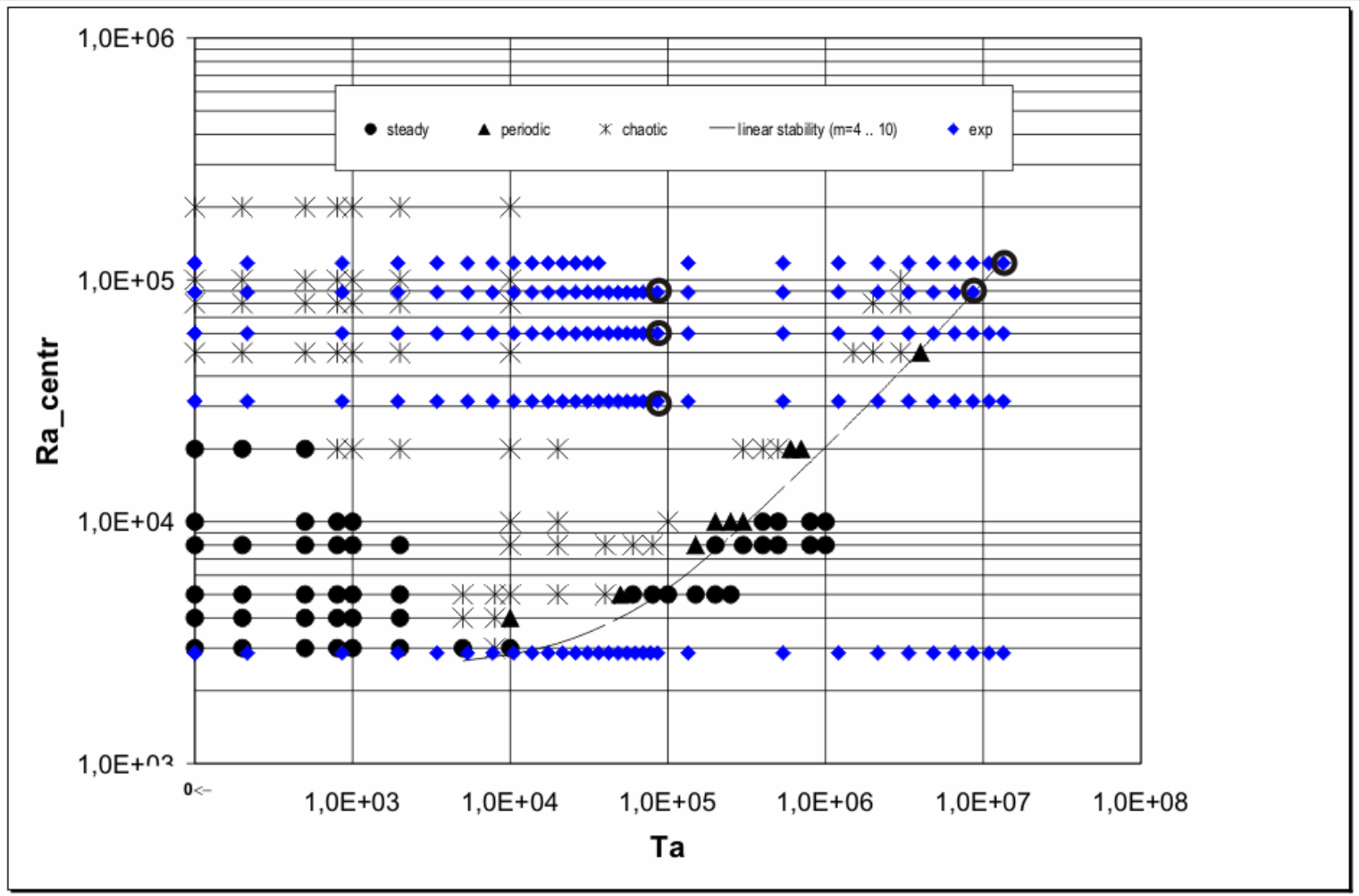

Patterns of convection in the rapid rotation regime: Alignment of convective cells at the tangent cylinder

$Ra_{centr} = 8.87 \cdot 10^4$
$Ta = 8.59 \cdot 10^6$

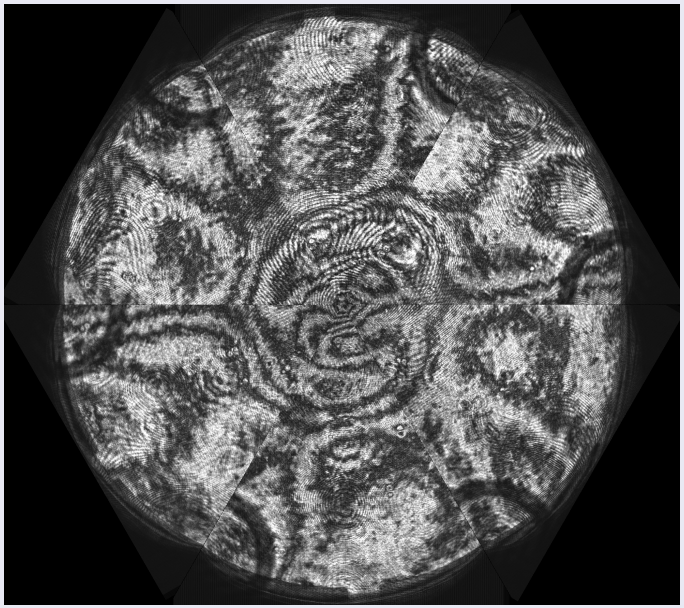

$Ra_{centr} = 1.17 \cdot 10^5$
$Ta = 1.34 \cdot 10^7$

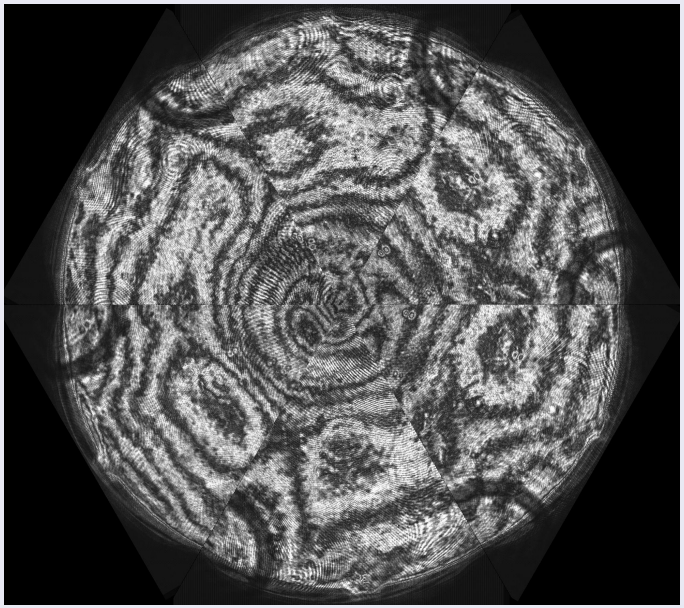

'columnar cells'

Patterns of convection in the moderate rotation regime:
Increase of thermal forcing leads to symmetry breaking bifurcations

$Ra_{centr} = 3.15 \cdot 10^4$
$Ta = 8.59 \cdot 10^4$

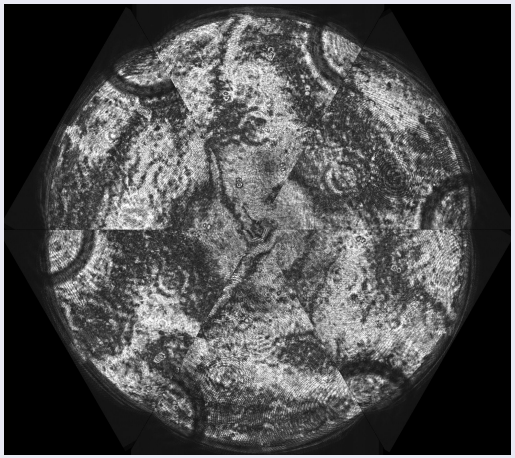

$Ra_{centr} = 6.01 \cdot 10^4$
$Ta = 8.59 \cdot 10^4$

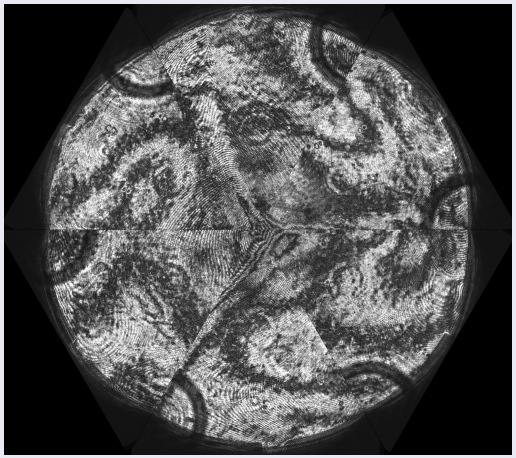

$Ra_{centr} = 8.87 \cdot 10^4$
$Ta = 8.59 \cdot 10^4$

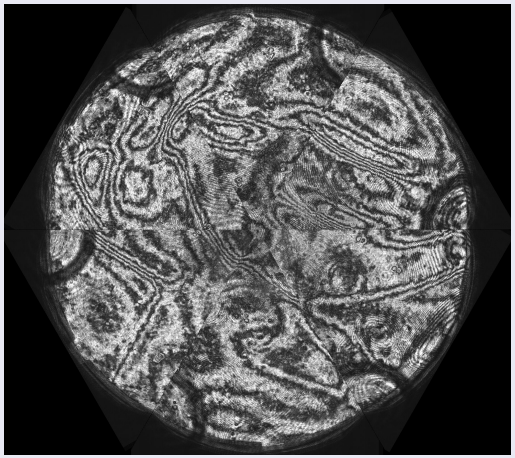

Patterns of convection visualized with fringes from Wollaston shearing interferometry

to be continued ...
with Part II: Steps of Numerical and Experimental Alignment

Global/local variables and patterns of convection for Ta low: $Ra_{centr} = 3 \cdot 10^3$, $Ta = 2 \cdot 10^2$

$E_{kin} = 72$

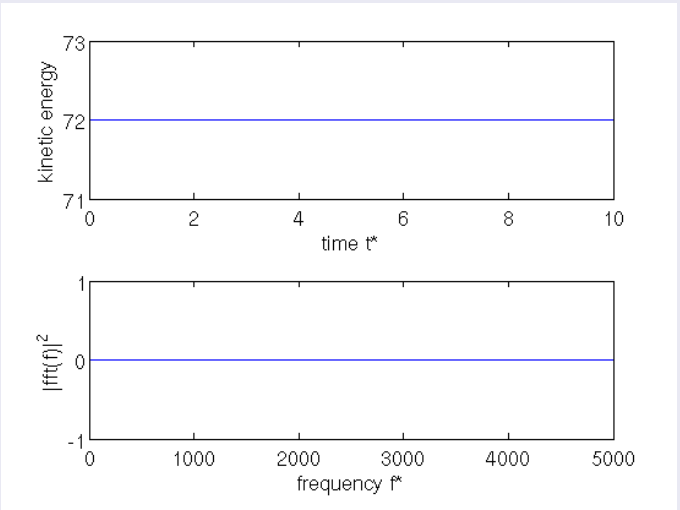

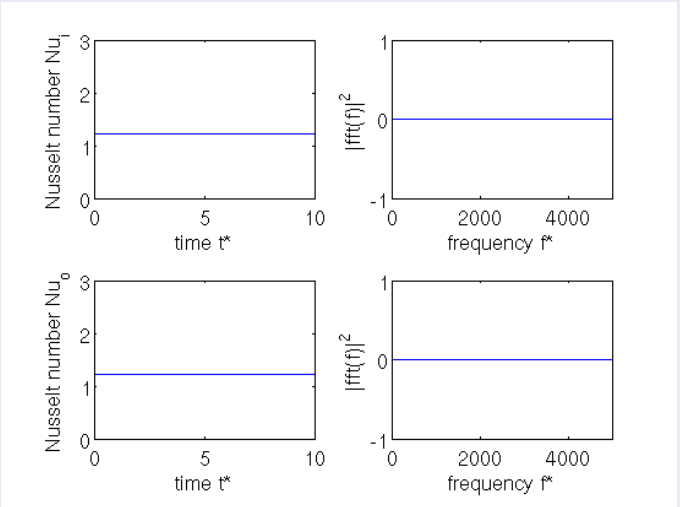

$Nu = 1.21530$

spect. coeff.

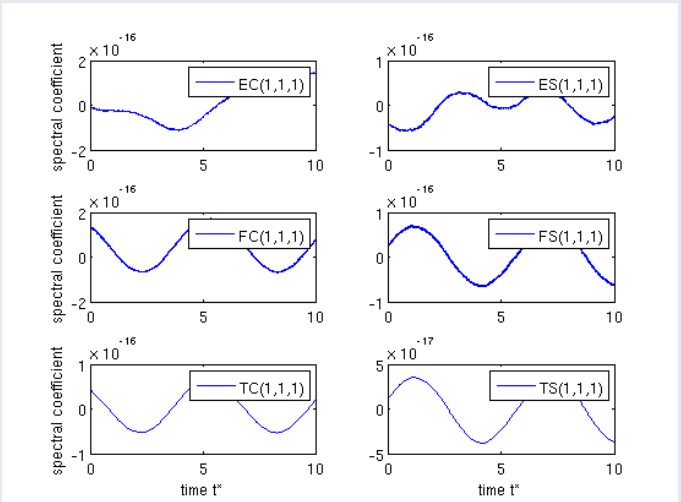

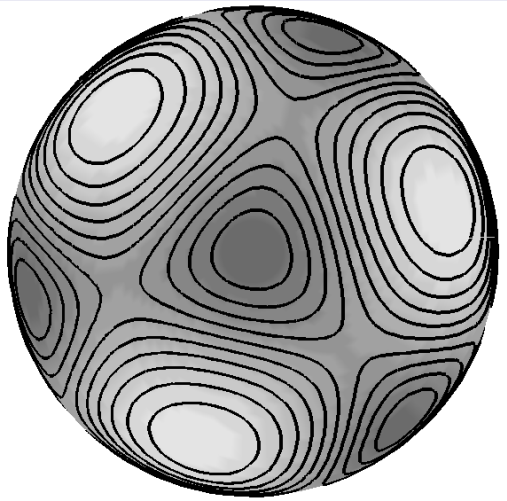

temp. pattern

Global/local variables and patterns of convection for Ta low: $Ra_{centr} = 3 \cdot 10^3$, $Ta = 1 \cdot 10^3$

$E_{kin} =$ 65

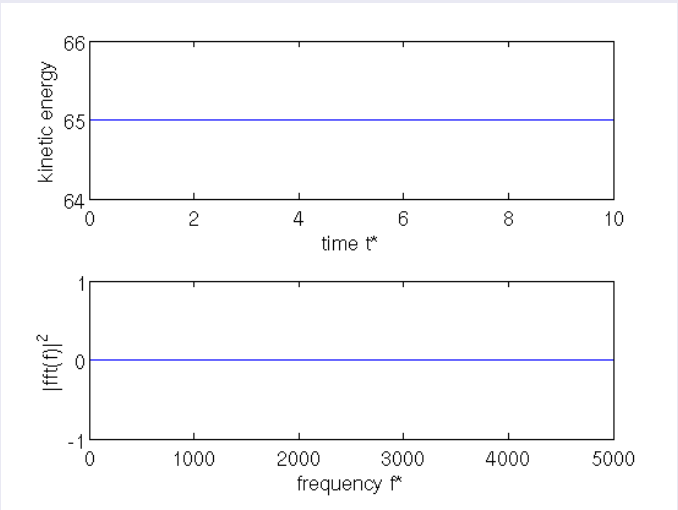

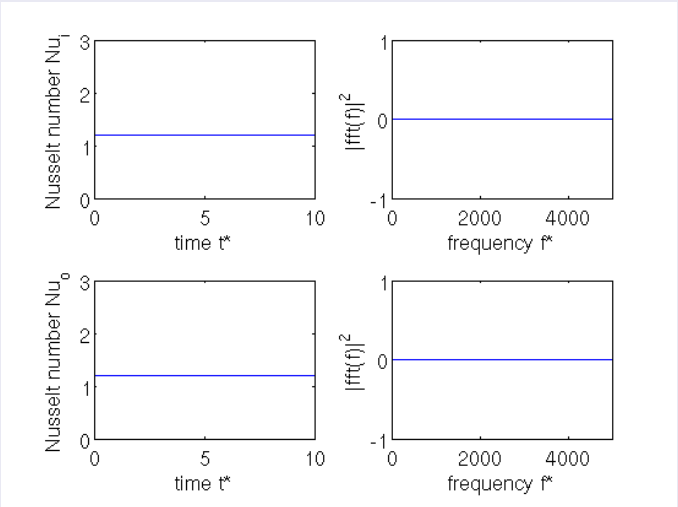

$Nu = 1.19666$

spect. coeff.

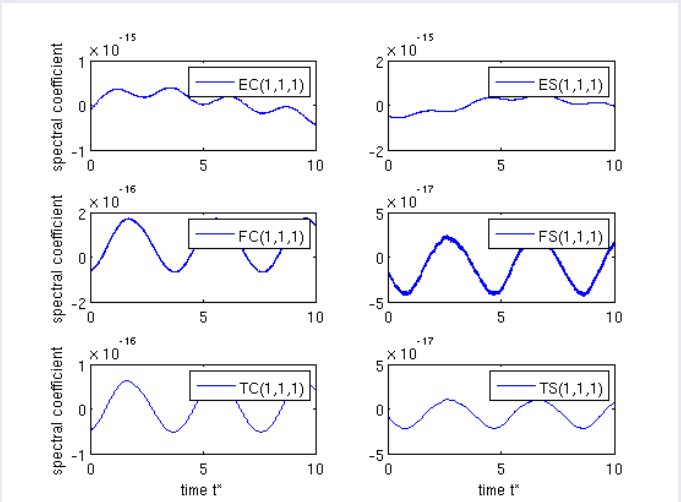

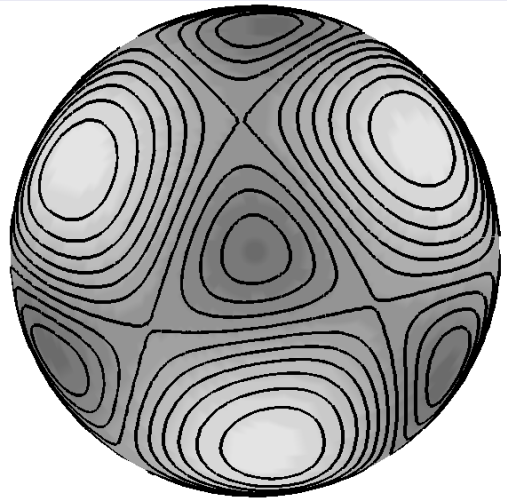

temp. pattern

Global/local variables and patterns of convection for Ta low: $Ra_{centr} = 5 \cdot 10^3,\ Ta = 2 \cdot 10^2$

$E_{kin} = 408$

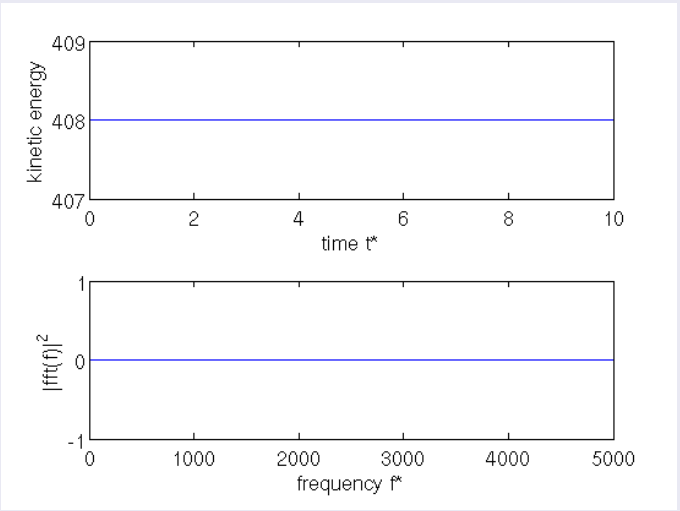

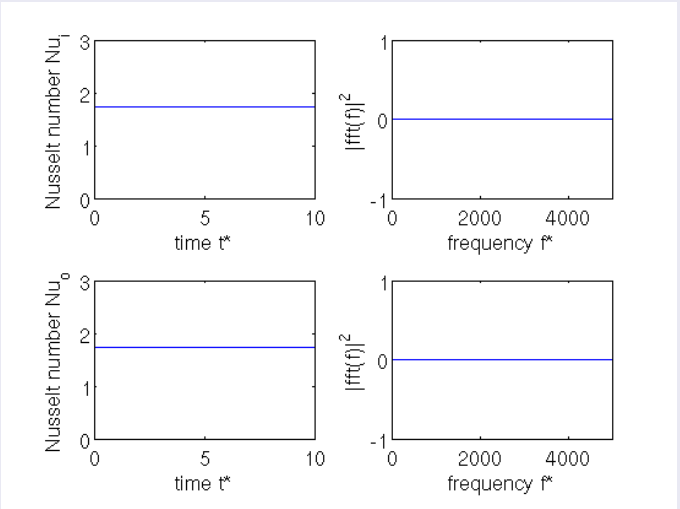

$Nu = 1.72162$

spect. coeff.

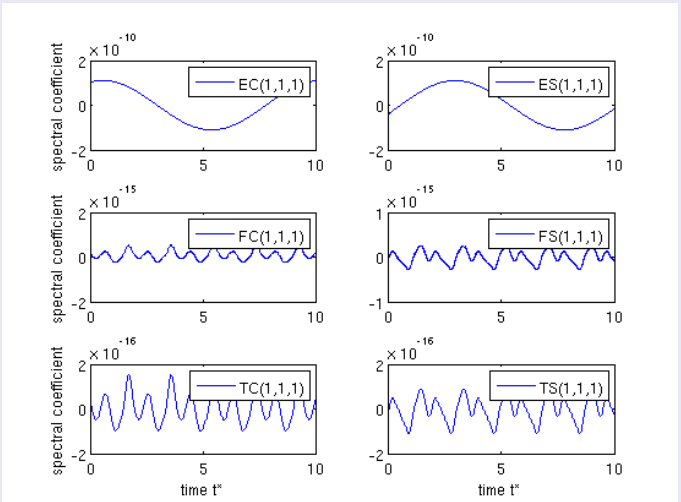

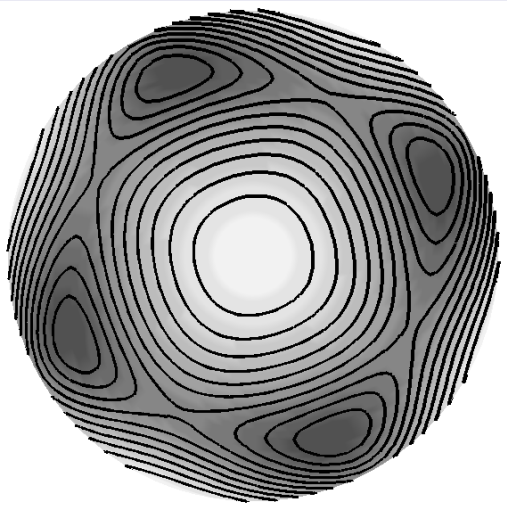

temp. pattern

Global/local variables and patterns of convection for Ta low: $Ra_{centr} = 5 \cdot 10^3$, $Ta = 1 \cdot 10^3$

$E_{kin} = 397$

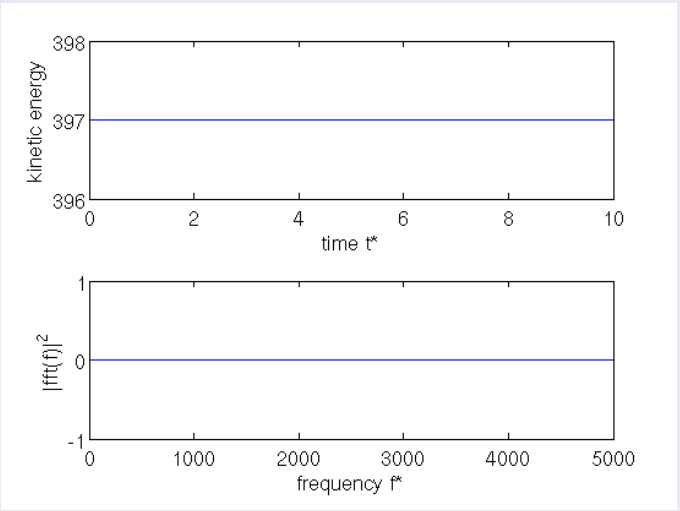

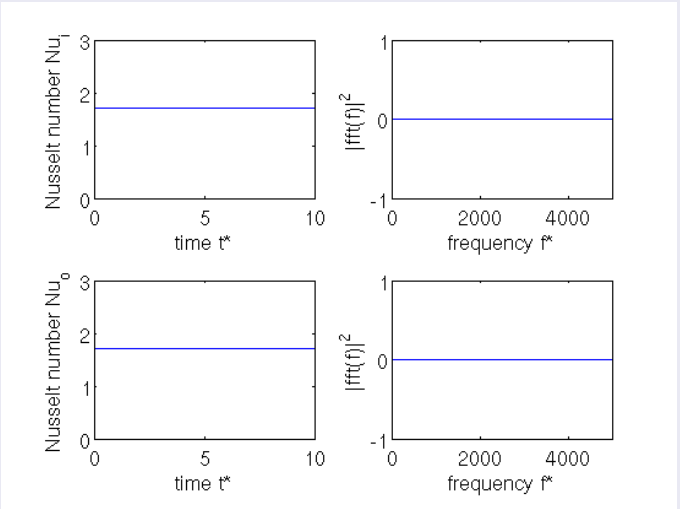

$Nu = 1.69827$

spect. coeff.

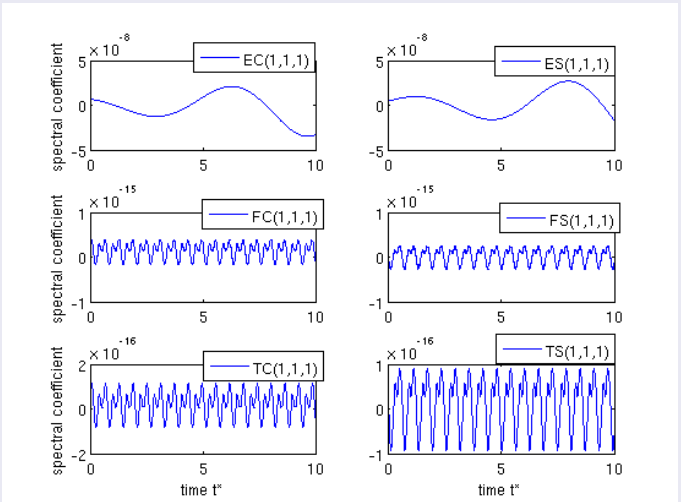

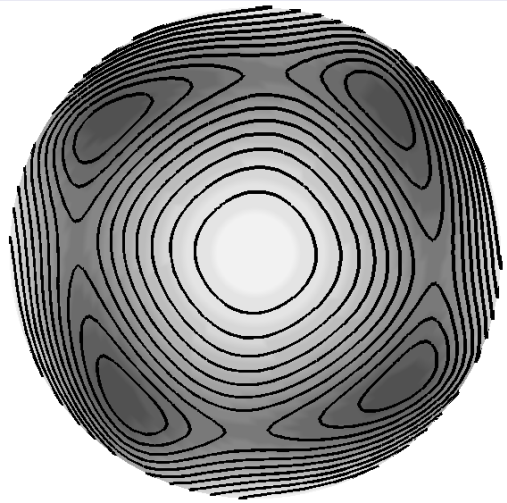

temp. pattern

Global variables for Ta low ($Ta \leq 10^4$

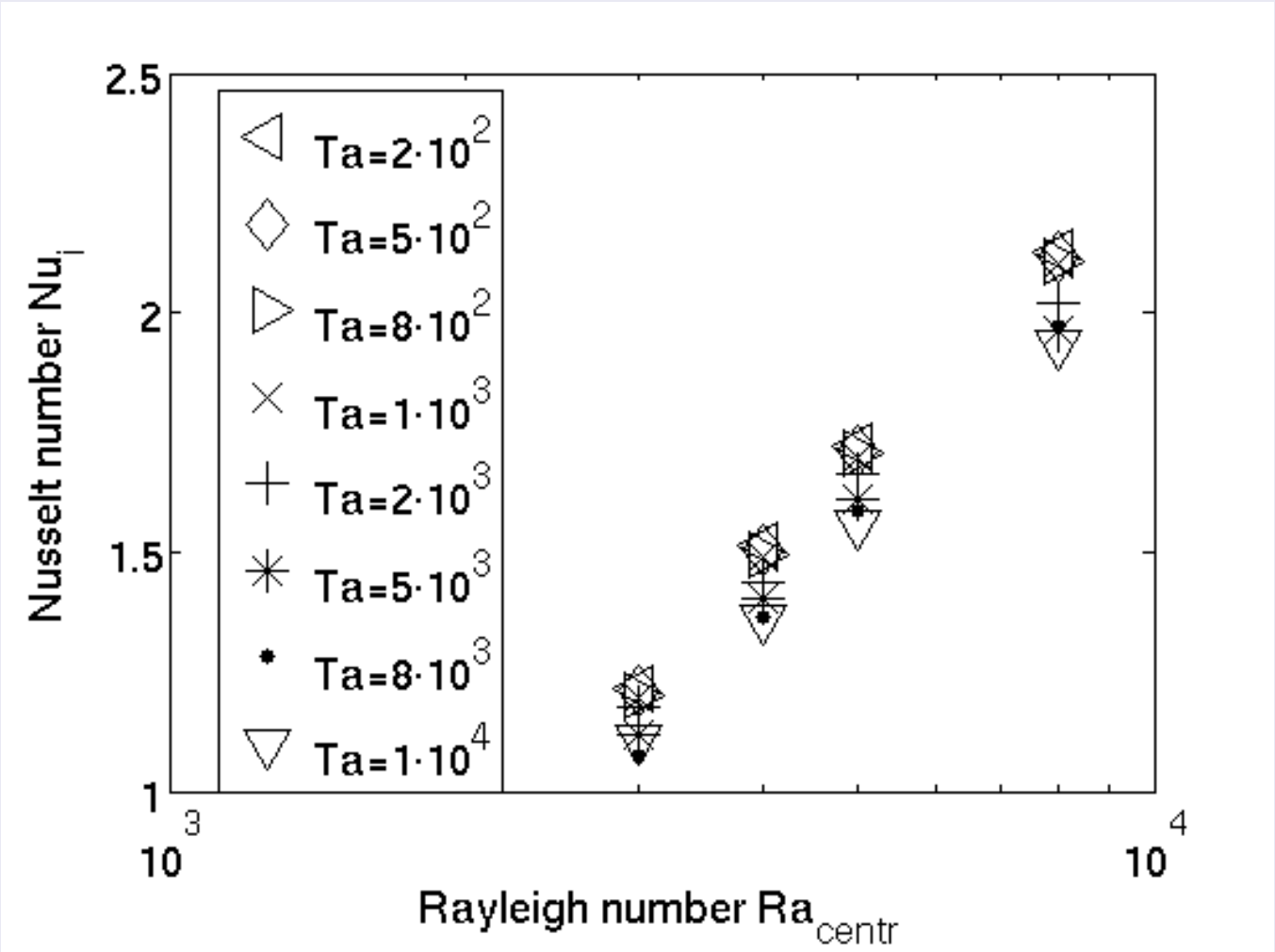

Global variables for Ta low ($Ta \leq 10^4$